Journal of Computational Physics **159,** 312–328 (2000)
doi:10.1006/jcph.2000.6447, available online at http://www.idealibrary.com on IDEAL®

Spectrum of Electrostatic Modes in a Cylindrical Non-neutral Plasma of Arbitrary Density

Priyanka Goswami,* S. N. Bhattacharyya,† and A. Sen‡

Institute for Plasma Research, Bhat, Gandhinagar 382428, India
E-mail: *priya@plasma.ernet.in, †snb@plasma.ernet.in, ‡abhijit@plasma.ernet.in

Received July 6, 1999; revised January 4, 2000

The eigenvalue problem governing small amplitude electrostatic modes in a cylindrical column of non-neutral plasma is solved using a finite difference method. The eigenvalue problem is considered as a system of differential equations. A finite difference approximation using a staggered grid converts this system to a generalized matrix eigenvalue problem which is solved using readily available library subroutines. Important features of the spectrum, such as degenerate eigenvalues, sequences of eigenvalues, continua, and unstable modes, are well represented by the method.

Key Words: non-neutral plasma; electrostatic modes; diocotron modes; continuous spectrum; surface modes; finite difference; staggered grid; non-self-adjoint eigenvalue problem.

1. INTRODUCTION

In recent years there has been considerable interest in computing the spectrum of electrostatic modes in magnetically confined non-neutral plasmas. While the low-frequency diocotron branch has been studied extensively, both analytically [1–5] and numerically [6–8], interest in the high-frequency cyclotron or upper hybrid branch is fairly recent [9–12]. To compare with the experimental observations [10], analytical solutions have been obtained for cyclotron modes in a low-density cylindrical column of non-neutral plasma [10–12]. These solutions are restricted to some particular choice of the equilibrium density profile. Analytical solutions have also been obtained for both branches of the electrostatic spectrum in a spheroidal non-neutral plasma [13]. These are again restricted by the assumption of a constant density profile. The frequencies of various modes in spheroidal non-neutral plasmas have been measured experimentally and these measurements have been used as non-destructive diagnostics for plasma parameters [14–16]. It has been recognized that deviations from the number density profile assumed in the analytical studies can cause quantitative changes in the mode frequencies [11]. Therefore, it appears relevant

0021-9991/00 $35.00

to develop a numerical code which can compute the entire spectrum of electrostatic modes for arbitrary profiles of the number density.

Recently a numerical code for computing mode frequencies in a non-neutral plasma has been developed [17]. This code allows arbitrary profiles of the number density and considers both the diocotron and the upper hybrid branch. However, the method used involves an extensive search of the frequency domain, which is expected to be computationally expensive. Computation of the mode frequencies was reported for configurations that are stable. Using this code, it would be even more difficult to predict instability, since this would involve a search in the complex frequency plane.

By contrast, in magnetohydrodynamics (MHD) codes have been developed which compute the entire spectrum of normal modes [18–22]. These codes use the finite element method to convert the differential equations governing linear stability to a generalized matrix eigenvalue problem. The eigensolutions can then be readily obtained using matrix eigenvalue solvers.

In this paper we develop a numerical code for computing the complete spectrum of electrostatic modes in a non-neutral plasma. For simplicity we consider a cylindrical equilibrium. We pattern our work on the lines of the stability codes in MHD. However, instead of the finite element method, we use the finite difference method.

While developing the stability codes in MHD some difficulties were encountered, e.g., spectral pollution. It was demonstrated that the problem could be resolved by an appropriate choice of basis functions in the finite element method [19]. Later it was shown that an alternative method for avoiding spectral pollution was by using what were termed "finite hybrid elements" [20]. This method uses the values of some variables at the mesh points and of the other variables at midpoints between mesh points. Although spectral pollution may not be a serious problem in the computation of the spectrum of a non-neutral plasma, it was realized that the use of a finite difference approximation with a staggered grid, which again uses the values of some variables at mesh points and of other variables at midpoints, provides a method to correctly take into account the appropriate boundary conditions.

The novel feature of the present numerical study is the use of a staggered grid and a suitable choice of which variables to define at grid points and which at midpoints. This allows us to convert the differential equations governing linear stability to a matrix eigenvalue problem which is linear in the eigenvalue and to develop codes for computing the entire spectrum of eigenmodes on the lines of the widely used spectral codes in MHD [21, 22]. As discussed in Section 3, the numerical method developed in this paper correctly addresses a tricky issue regarding the appropriate boundary conditions for the problem.

It should be noticed that, while linear MHD stability is governed by a self-adjoint eigenvalue problem, the equations governing small amplitude electrostatic modes in a non-neutral plasma constitute a non-self-adjoint system. While solutions have been obtained for the non-self-adjoint eigenvalue problem governing resistive MHD stability [23], it is recognized that the non-symmetric eigenvalue problem is still by no means standard [24]. Therefore, it would be of interest to demonstrate the feasibility of solving the non-self-adjoint eigenvalue problem for electrostatic modes in a non-neutral plasma.

This paper is arranged in the following manner. In Section 2 we formulate the problem of linear stability to electrostatic modes in a cylindrical geometry. In Section 3 we develop the numerical procedure for computing the spectrum and in Section 4 we use this procedure to compute the spectrum for some specific choice of the number density profile. In Section 5 we discuss our findings and identify areas for further work.

2. MATHEMATICAL FORMULATION

We consider a single species non-neutral plasma in an externally imposed magnetic field. We assume that relativistic and plasma diamagnetic effects can be neglected and furthermore consider only electrostatic modes. Then, assuming a cold fluid model, the governing equations are [25]

$$\frac{\partial n}{\partial t} + \nabla \cdot (n\mathbf{v}) = 0, \tag{1}$$

$$\frac{\partial \mathbf{v}}{\partial t} + \mathbf{v} \cdot \nabla \mathbf{v} = \frac{q}{m}(-\nabla\varphi + \mathbf{v} \times \mathbf{B}), \tag{2}$$

$$\nabla^2\varphi = -\frac{q}{\epsilon_0} n. \tag{3}$$

Here n and $\mathbf{v}$ are the number density and fluid velocity of the plasma, q and m are the charge and mass of each particle of the plasma, φ is the electrostatic potential, $\mathbf{B}$ is the externally imposed magnetic field, and ϵ_0 is the permittivity of free space. We now transform to dimensionless variables. We scale coordinates, number density, and magnetic field with respect to reference values a, n_0, and B_0. We choose a to be the radius of the cylindrical wall enclosing the plasma; n_0 to be the number density of the plasma on the axis, or, for an annular plasma, to be the number density at some specified radial location; and B_0 to be the axial magnetic field. Furthermore, we scale φ, $\mathbf{v}$, and t relative to $\varphi_0 = qn_0a^2/\epsilon_0$, $v_0 = |\varphi_0|/aB_0$, and $t_0 = a/v_0$. In terms of dimensionless variables Eqs. (1)–(3) are

$$\frac{\partial n}{\partial t} + \nabla \cdot (n\mathbf{v}) = 0, \tag{4}$$

$$M\left(\frac{\partial \mathbf{v}}{\partial t} + \mathbf{v} \cdot \nabla \mathbf{v}\right) = -\nabla\varphi + \epsilon \mathbf{v} \times \mathbf{B}, \tag{5}$$

$$\nabla^2\varphi = -n. \tag{6}$$

Here $\epsilon = |q|/q$ is the sign of the charge on each particle of the plasma and

$$M = \frac{\omega_{p0}^2}{\omega_c^2}, \tag{7}$$

where $\omega_{p0}^2 = q^2n_0/\epsilon_0 m$ and $\omega_c = |q|B_0/m$ are the square of the plasma frequency and the cyclotron frequency, respectively. It is readily seen that $t_0 = \omega_c/\omega_{p0}^2$. Therefore, the frequency scale is twice the diocotron frequency.

We consider a cylindrical equilibrium confined by an axial magnetic field. In a cylindrical coordinate system (r, θ, z) we assume that the magnetic field in dimensionless variables is $\mathbf{B} = \mathbf{e}_z$. We assume an equilibrium given by

$$n = n^0(r), \qquad \mathbf{v} = r\omega_r(r)\mathbf{e}_\theta, \qquad \varphi = \varphi^0(r). \tag{8}$$

The equation governing equilibrium is [26]

$$M\omega_r^2 + \epsilon\omega_r + \frac{1}{r^2}\int_0^r n^0(r')r'\,dr' = 0. \tag{9}$$

We next consider a perturbation from this equilibrium given by

$$n = n^0 + \delta n, \qquad \mathbf{v} = \delta v_r \mathbf{e}_r + (r\omega_r + \delta v_\theta)\mathbf{e}_\theta + \delta v_z \mathbf{e}_z, \qquad \varphi = \varphi^0 + \delta\varphi. \tag{10}$$

The linearized equations for perturbations with (t, θ, z)-dependence of the form $\exp[i(l\theta + kz - \omega t)]$ are [27]

$$-Mi(\omega - l\omega_r)\delta v_r - (\epsilon + 2M\omega_r)\delta v_\theta = -\frac{d}{dr}\delta\varphi, \tag{11}$$

$$-Mi(\omega - l\omega_r)\delta v_\theta + \left(\epsilon + 2M\omega_r + Mr\frac{d\omega_r}{dr}\right)\delta v_r = -\frac{il}{r}\delta\varphi, \tag{12}$$

$$-Mi(\omega - l\omega_r)\delta v_z = -ik\delta\varphi, \tag{13}$$

$$i(\omega - l\omega_r)\left[\frac{1}{r}\frac{d}{dr}\left(r\frac{d}{dr}\delta\varphi\right) - \frac{l^2}{r^2}\delta\varphi - k^2\delta\varphi\right] + \frac{1}{r}\frac{d}{dr}\left(rn^0\delta v_r\right) + n^0\frac{il}{r}\delta v_\theta + n^0 ik\delta v_z = 0. \tag{14}$$

We assume a grounded conducting wall at $r = 1$. Then $\varphi = 0$ at $r = 1$. The appropriate boundary condition on the perturbation is

$$\delta\varphi = 0 \qquad \text{at } r = 1. \tag{15}$$

Solving for δv_r, δv_θ, and δv_z in terms of $\delta\varphi$ from Eqs. (11)–(13) and substituting in Eq. (14), we obtain

$$\frac{1}{r}\frac{d}{dr}\left[r\left(1 - \frac{Mn^0}{G}\right)\frac{d}{dr}\delta\varphi\right] - \frac{l^2}{r^2}\left(1 - \frac{Mn^0}{G}\right)\delta\varphi - k^2\left[1 - \frac{n^0}{M(\omega - l\omega_r)^2}\right]\delta\varphi + \frac{1}{(\omega - l\omega_r)}\frac{l}{r}\delta\varphi\frac{d}{dr}\left[\frac{n^0}{G}(\epsilon + 2M\omega_r)\right] = 0, \tag{16}$$

where

$$G = M^2(\omega - l\omega_r)^2 - (\epsilon + 2M\omega_r)\left(\epsilon + 2M\omega_r + Mr\frac{d\omega_r}{dr}\right). \tag{17}$$

Equation (16), together with boundary condition (15) and the condition of regularity of the solution at $r = 0$, constitutes an eigenvalue problem for ω. Once the eigenfunction $\delta\varphi$ is known, δv_r, δv_θ, and δv_z can be obtained by algebraically solving Eqs. (11)–(13). Since no derivatives of these variables are involved, the solutions for δv_r, δv_θ, and δv_z can be obtained without requiring any boundary conditions on these variables. The entire eigensolution can be obtained using only boundary condition (15). Therefore Eq. (15) is the only boundary condition required for Eqs. (11)–(14).

For a plasma column of constant density extending up to the wall, $n^0 = 1$ for $0 \le r \le 1$, the eigenvalue problem has an analytical solution [28]

$$\delta\varphi = AJ_l(Tr), \tag{18}$$

where A is a constant, J_l is the Bessel function of the first kind of order l, and

$$T^2 = -k^2 \frac{\left[1 - \frac{1}{M(\omega - l\omega_r)^2}\right]}{\left(1 - \frac{M}{G}\right)}, \tag{19}$$

where

$$G = M^2(\omega - l\omega_r)^2 - (\epsilon + 2M\omega_r)^2. \tag{20}$$

The dispersion relation is given by

$$T = p_{lm}, \qquad m = 1, 2, \ldots, \tag{21}$$

where p_{lm} is the mth zero of $J_l(x) = 0$. Using Eqs. (19) and (20), and with a little algebra, we obtain

$$M^3(\omega - l\omega_r)^4 - M\{(\epsilon + 2M\omega_r)^2 + M\}(\omega - l\omega_r)^2 + \frac{k^2}{k^2 + p_{lm}^2}(\epsilon + 2M\omega_r)^2 = 0. \tag{22}$$

For a non-constant density profile it is known that there exist two continuous spectra given by [29]

$$\omega - l\omega_r = 0, \tag{23}$$

$$M^2(\omega - l\omega_r)^2 - (\epsilon + M\omega_r)^2 - (M\omega_r)^2 = 0. \tag{24}$$

For a plasma column of constant density, separated by a vacuum region from the wall, described by the density profile

$$n^0 = \begin{cases} \bar{n}^0, & 0 \le r \le r_p, \\ 0, & r_p < r \le 1, \end{cases} \tag{25}$$

where $\bar{n}^0 = \text{const.}$, in addition to two infinitely degenerate points in the spectrum corresponding to the resonance conditions given by Eqs. (23) and (24), there are two surface waves which, for $k = 0$, are given by [30]

$$\omega = -\frac{\epsilon}{2M} + (l-1)\omega_r \pm \frac{1}{2M}\left(1 - 2M\bar{n}^0 r_p^{2l}\right)^{1/2}. \tag{26}$$

3. NUMERICAL PROCEDURE

For an arbitrary profile of the number density n^0 the eigenvalue problem has to be solved numerically. One approach is to solve Eq. (16), with boundary condition (15) and the condition of regularity at $r = 0$, using the finite difference method. This leads to a coefficient matrix which is nonlinear in ω. In Ref. [17], a nonhomogeneous source term was introduced in Eq. (16). The mode frequencies were determined by varying ω, solving the nonhomogeneous equation, and finding values of ω which make the solution infinite (or at least very large). In Ref. [17] the search involved 1200 different values of ω. Alternatively, one can use an iterative method for computing the eigenvalues of the homogeneous

problem. Such a method has been used in MHD [31]. It is recognized that this iterative method for solving a nonlinear eigenvalue problem requires more computation time compared to a procedure that involves solving a matrix eigenvalue problem which is linear in the eigenvalue ω.

We can obtain a matrix eigenvalue problem which is linear in ω by using finite difference approximations in Eqs. (11)–(14). We observe that Eq. (14) involves a derivative of δv_r. Does this require a boundary condition on δv_r? At first glance it might appear that $\delta v_r = 0$ would be an appropriate boundary condition at a rigid boundary at $r = 1$. However, in the previous section we observed that δv_r could be calculated without using any boundary condition on δv_r. Furthermore, for the constant density profile

$$\delta v_r = [Mi(\omega - l\omega_r)AT\ J_l'(Tr) + (\epsilon + 2M\omega_r)(il/r)AJ_l(Tr)]/G,$$

which does not vanish at $r = 1$. Furthermore, for the mode $l = 1$, it is readily seen that $\delta v_r,\ \delta v_\theta \neq 0$ at $r = 0$. To avoid these difficulties we choose a finite difference scheme which does not involve the values of δv_r and δv_θ at $r = 0$ and 1. We define a set of equispaced grid points $r_i = i/N,\ i = 0, 1, \ldots, N$. For each interval $[r_{i-1}, r_i]$ we define the midpoint by $r_{i-1/2} = (r_{i-1} + r_i)/2$. For Eqs. (11) and (12) we use finite difference approximations at the midpoints $r = r_{i-1/2}, i = 1, \ldots, N$, while for Eqs. (13) and (14) we use finite difference approximations at the grid points $r = r_i, i = 1, \ldots, N - 1$. We obtain

$$\begin{aligned} &Ml\omega_{r,i-1/2}u_{i-1/2} + (\epsilon + 2M\omega_{r,i-1/2})v_{i-1/2} - \frac{f_i - f_{i-1}}{h} \\ &\quad = \omega M u_{i-1/2}, \qquad i = 1, \ldots, N, \end{aligned} \tag{27}$$

$$\begin{aligned} &Ml\omega_{r,i-1/2}v_{i-1/2} + \left(\epsilon + 2M\omega_{r,i-1/2} + Mr_{i-1/2}\frac{\omega_{r,i} - \omega_{r,i-1}}{h}\right)u_{i-1/2} \\ &\quad + \frac{l}{r_{i-1/2}}\frac{1}{2}(f_{i-1} + f_i) = \omega M v_{i-1/2}, \qquad i = 1, \ldots, N, \end{aligned} \tag{28}$$

$$Ml\omega_{r,i}w_i + kf_i = \omega M w_i, \qquad i = 1, \ldots, N - 1, \tag{29}$$

$$\begin{aligned} &l\omega_{r,i}\left[\frac{-r_{i-1/2}f_{i-1} + 2r_i f_i - r_{i+1/2}f_{i+1}}{h^2} + \frac{l^2}{r_i}f_i + k^2 r_i f_i\right] \\ &\quad + \frac{r_{i+1/2}n_{i+1/2}^0 u_{i+1/2} - r_{i-1/2}n_{i-1/2}^0 u_{i-1/2}}{h} + n_i^0 l\frac{1}{2}(v_{i+1/2} + v_{i-1/2}) + n_i^0 k r_i w_i \\ &= \omega\left[\frac{-r_{i-1/2}f_{i-1} + 2r_i f_i - r_{i+1/2}f_{i+1}}{h^2} + \frac{l^2}{r_i}f_i + k^2 r_i f_i\right], \qquad i = 1, \ldots, N - 1. \end{aligned} \tag{30}$$

Here $u = \delta v_r, v = i\delta v_\theta, w = i\delta v_z, f = i\delta\varphi$, and subscripts $i, i - \frac{1}{2}$, etc., denote values at grid points and midpoints. The error in the finite difference approximations in Eqs. (27)–(30) is $\mathcal{O}(h^2)$. Equations (27)–(30) can be written in the form

$$\mathbf{Ax} = \omega\mathbf{Bx}, \tag{31}$$

where $\mathbf{x}$ is a vector of dimension $4N-2$ defined by

$$\mathbf{x} = [u_{1/2}\ v_{1/2}\ w_1\ f_1\ u_{3/2}\ v_{3/2}\ \cdots\ w_{N-1}\ f_{N-1}\ u_{N-1/2}\ v_{N-1/2}]^T;$$

the superscript T denotes the transpose, and $\mathbf{A}$ and $\mathbf{B}$ are $(4N-2)\times(4N-2)$ real matrices. Equation (31) is solved using readily available library subroutines.

In a non-neutral plasma equilibrium, as in MHD equilibria, the region inside the enclosing wall can contain vacuum regions as well as regions containing plasma. In numerical computations of the MHD spectrum [21, 22], a separate analysis is carried out for the vacuum region. In a non-neutral plasma the appropriate equation in the vacuum region is

$$\frac{1}{r}\frac{d}{dr}\left(r\frac{d}{dr}\delta\varphi\right) - \frac{l^2}{r^2}\delta\varphi - k^2\delta\varphi = 0,$$

and δv_r, δv_θ, and δv_z have no meaning in the vacuum region. To satisfy these conditions, for points in the vacuum we artificially set all terms on the left-hand side of Eqs. (27)–(30) to zero. Then for modes with $\omega \neq 0$ the numerical solution satisfies

$$\begin{aligned} Mu_{i-1/2} &= 0,\\ Mv_{i-1/2} &= 0,\\ Mw_i &= 0,\\ \left[\frac{-r_{i-1/2}f_{i-1} + 2r_i f_i - r_{i+1/2}f_{i+1}}{h^2} + \frac{l^2}{r_i}f_i + k^2 r_i f_i\right] &= 0, \end{aligned}$$

for points in the vacuum, which is consistent with the governing equations in the vacuum region. The last equation is readily seen to be the finite difference representation of the equation for $\delta\varphi$. The numerical scheme also yields a number of modes with $\omega = 0$, which may not satisfy the correct governing equations in the vacuum region. We ignore these modes. This method of accounting for the vacuum region will encounter problems if the configuration has natural modes with $\omega = 0$. In such a case we should write the finite difference equation for $\delta\varphi$ in the vacuum region. These equations do not involve ω and, therefore, can be solved for $\delta\varphi$ in the vacuum region in terms of $\delta\varphi$ in the plasma region. Substituting this in the finite difference equations in the plasma region we obtain a matrix eigenvalue problem of reduced size. All eigensolutions, including any modes with $\omega = 0$, are valid eigenmodes of the physical system. In our study, to account for the vacuum region, we have used the method described first.

4. APPLICATIONS

In this section we use the numerical method developed in the previous section to compute the spectrum of electrostatic modes for a few test cases.

4.1. *Constant Density Profile*

As a first test case we consider a plasma column of constant density extending up to the wall

$$n^0 = 1 \qquad \text{for } 0 \le r \le 1. \tag{32}$$

Using Eq. (9) we easily see that the rotation frequency is given by

$$\omega_r = \frac{-\epsilon \pm \sqrt{1-2M}}{2M}.$$

The two signs represent the slow and fast rotational equilibria. In our numerical study we will consider only the slow rotational equilibrium. This constant density plasma column is the counterpart of the homogeneous currentless plasma cylinder in MHD and the spectrum can contain infinitely degenerate eigenvalues. In MHD it was demonstrated that an inappropriate choice of basis functions in the finite element method can destroy the degeneracy [32]. Two methods were suggested for preserving the degeneracy [19, 20]. For a non-neutral plasma if $k=0$ the spectrum contains the degenerate diocotron frequency

$$\omega = l\omega_r, \tag{33}$$

and the degenerate upper hybrid frequencies

$$\omega = l\omega_r \pm \frac{\left[(\epsilon + M\omega_r)^2 + (M\omega_r)^2\right]^{1/2}}{M}. \tag{34}$$

Numerical computation was carried out for various values of M. For N grid intervals the diocotron frequency is obtained with $2(N-1)$-fold degeneracy and each branch of the upper hybrid frequency with $(N-1)$-fold degeneracy. In addition, we obtain two eigenfrequencies given by

$$\omega = l\omega_r \pm \frac{(\epsilon + 2M\omega_r)}{M}. \tag{35}$$

For these two modes the eigenfunctions have $\delta v_z = \delta\varphi = 0$. It can be verified analytically, using Eqs. (11)–(14), that these represent valid eigensolutions and are not spurious modes.

For $k \neq 0$ for the special case $M=0.5$ the spectrum again contains degenerate points which are given correctly by the numerical method. For $k \neq 0$, $M \neq 0.5$ there are sequences of eigenvalues representing the diocotron and the upper hybrid frequencies. For $M=0.4$ and $\epsilon = 1$, the spectrum for the modes $l=1$, and for a few values of k between 0 and 2π, computed using 40 grid intervals, is shown in Fig. 1. The two bands in the middle represent the diocotron branch. These two bands start from the fundamental modes at $\omega = -1.563652$ and $\omega = 0.182186$ for $k = 2\pi$ and extend toward an accumulation point at $\omega = -0.690983$. The two bands at the top and the bottom represent the upper hybrid branch. For comparison the eigenfrequencies computed using the analytical dispersion relation, Eq. (22), are also plotted in Fig. 1. The numerical and analytical results show very good agreement. Comparing the numbers we find that for each branch of the dispersion relation the frequency of the fundamental mode agrees to three decimal places while frequencies of the first 10 modes in each branch agree to 1%. The accuracy of the finite difference method can be significantly further improved using Richardson extrapolation. In Fig. 2 we plot the eigenfunction $\delta\varphi$, computed using the finite difference method, for two different eigenfrequencies, which again show very good agreement with the analytical expression for the eigenfunction given by Eq. (18).

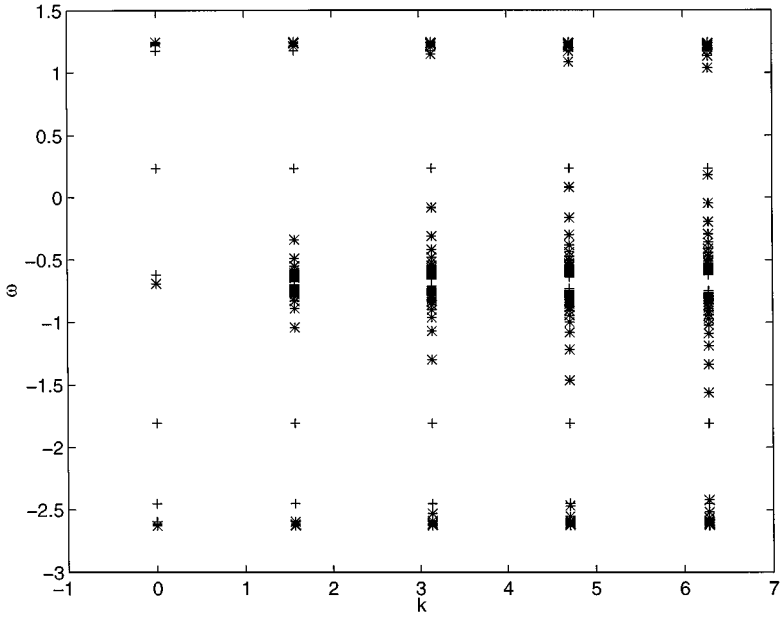

FIG. 1. The spectrum of the mode $l = 1$, for a constant density profile with $M = 0.4$ and $\epsilon = 1$: (+) numerical values; (×) analytical values.

4.2. *Continuously Varying Monotone Decreasing Density Profile*

We next consider the density profile

$$n^0 = 1 - r^2 \qquad \text{for } 0 \le r \le 1. \tag{36}$$

Using Eq. (9) we obtain

$$\omega_r = \frac{-\epsilon \pm \sqrt{1 - 2M(1 - r^2/2)}}{2M}.$$

The spectrum is computed for $M = 0.5$, $\epsilon = 1$, and $k = 0$. For the mode $l = 1$ the spectrum is shown in Fig. 3. It is seen to contain three bands of eigenfrequencies that agree well with the analytical limits $-1 \le \omega \le -0.292893$ for the diocotron continuum given by Eq. (23), and $-2.414214 \le \omega \le -2.024944$ and $0.414214 \le \omega \le 1.439157$ for the upper hybrid continua given by Eq. (24). This confirms the prediction of Ref. [29], that of the three singularities in Eq. (16) only two give rise to continuous spectra. From Fig. 3 we also observe that apart from the continuous spectra there are also two discrete modes, a diocotron mode and an upper hybrid mode. For a mode in the upper hybrid continuum the electrostatic potential $\delta\varphi$ is shown in Fig. 4. It is seen that $\delta\varphi$ vanishes outside the resonant layer. This confirms an earlier conjecture that for $l = 1$ the upper hybrid branch contains a continuum of singular eigenmodes but these have no electric field exterior to the plasma and therefore are not observable, or excitable, with electrodes exterior to the plasma [12]. We also compute the spectrum for $l = 2$ and obtain continua which agree with analytical predictions. For a mode in the diocotron continuum, $\delta\varphi$ and $d\delta\varphi/dr$ are shown in Fig. 5, while for a mode in the upper hybrid continuum, $\delta\varphi$ is shown in Fig. 6. The singularities in the eigenfunctions agree with analytical predictions [29].

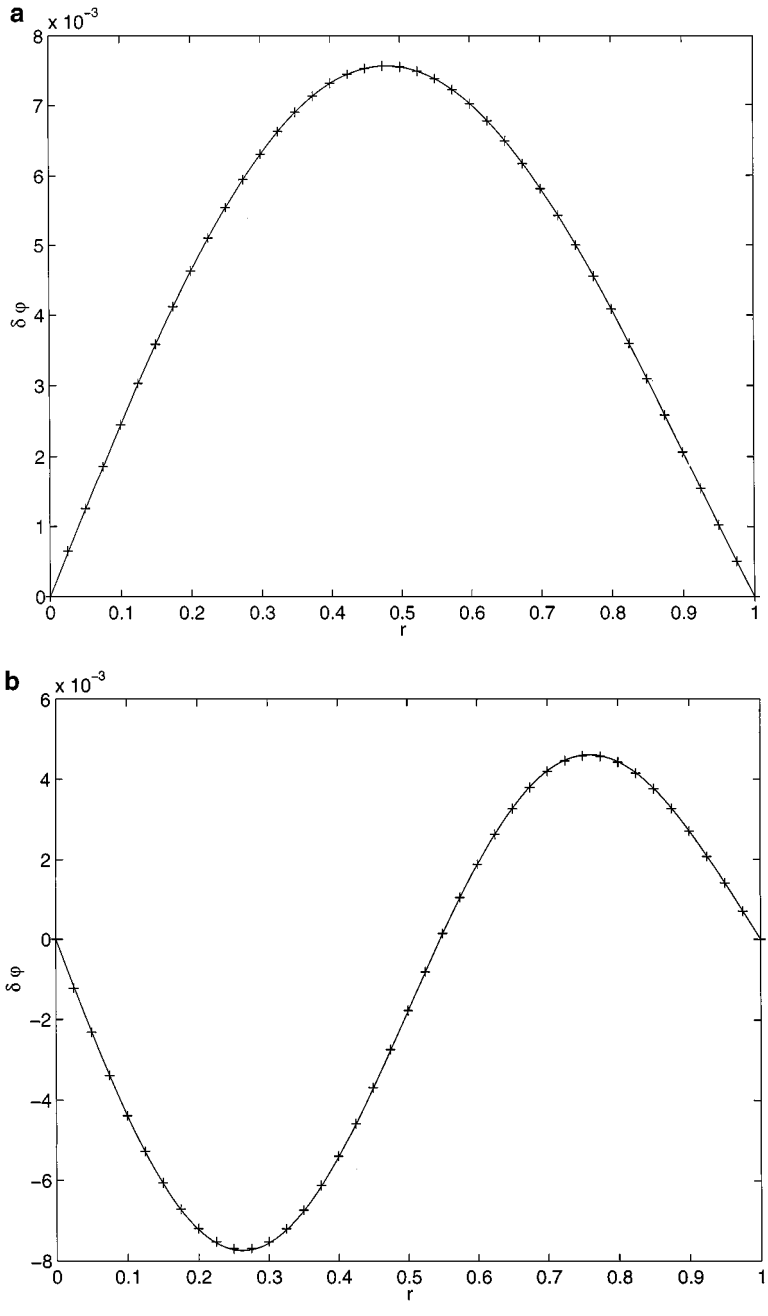

FIG. 2. Eigenfunction of the mode $l=1$, $k=0$ for a constant density profile for (a) $\omega=0.18218$ and (b) $\omega=-0.04459$: (+) numerical values; (—) analytical values.

4.3. *Surface Waves*

We now consider the density profile

$$n^0=\begin{cases} n_0(1-\mu r^2), & 0\le r\le r_p,\\ 0, & r_p<r\le 1,\end{cases} \tag{37}$$

where n_0 and μ are constants. We choose $n_0=1/(r_p^2-\frac{1}{2}\mu r_p^4)$ so that the total number per

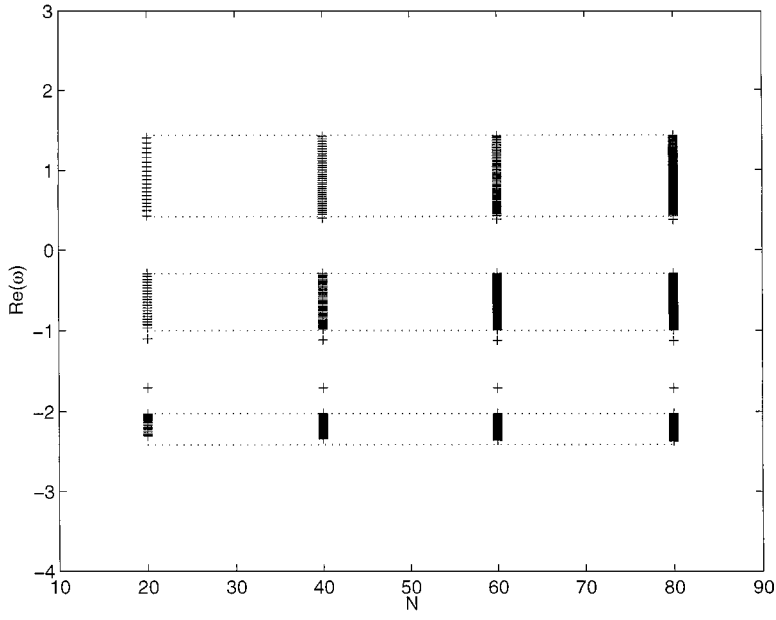

FIG. 3. The spectrum of the mode $l = 1, k = 0$ for a continuously varying monotone decreasing density profile with $M = 0.5$ and $\epsilon = 1$.

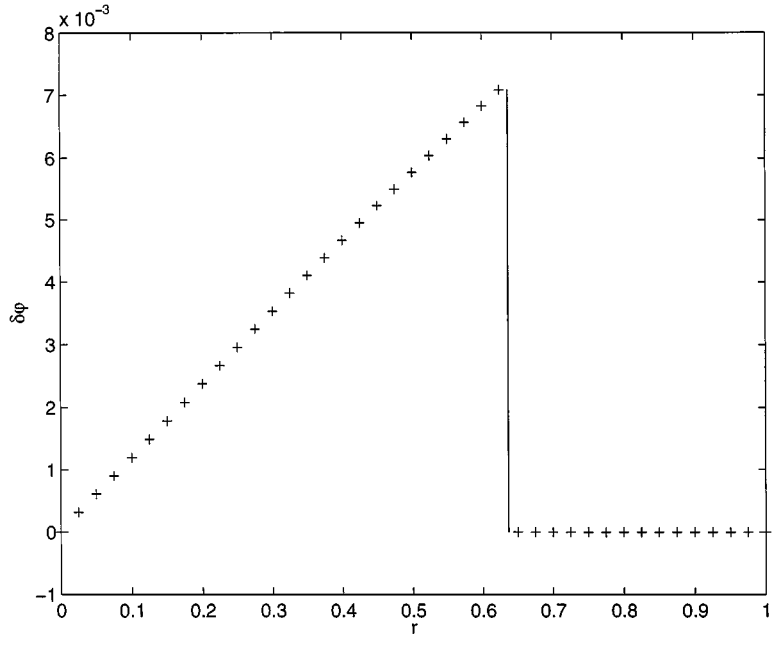

FIG. 4. Eigenfunction for $l = 1$ and $\omega = 1.00208$.

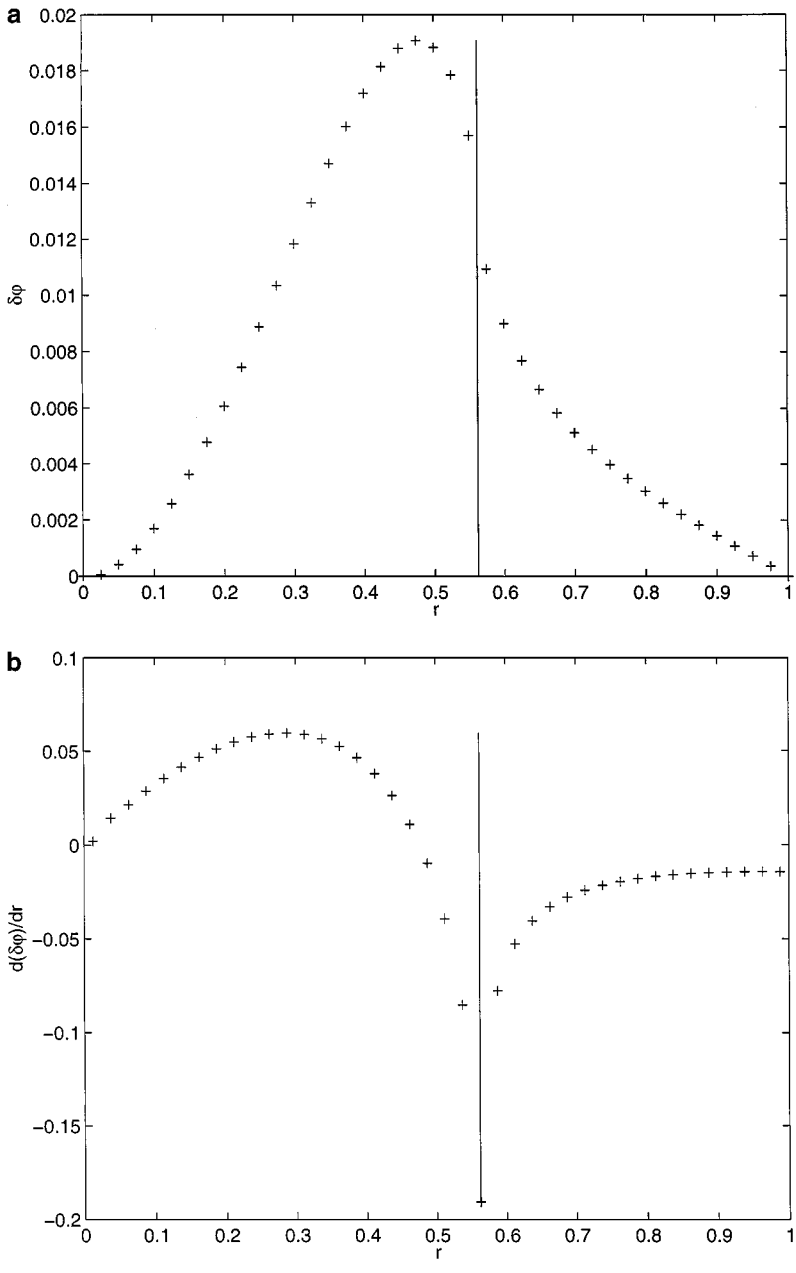

FIG. 5. (a) Eigenfunction and (b) derivative of the Eigenfunction for mode $l = 2$ and $\omega = -1.20081$.

unit length is the same for all values of μ and r_p. In the plasma region $0 \leq r \leq r_p$ the rotation frequency is given by

$$\omega_r = \frac{-\epsilon \pm \sqrt{1 - 2Mn_0(1 - \mu r^2/2)}}{2M}.$$

For $r_p = 0.5$, $\epsilon = 1$, and $M = 0.1$ the frequencies of the surface modes with $k = 0$ and

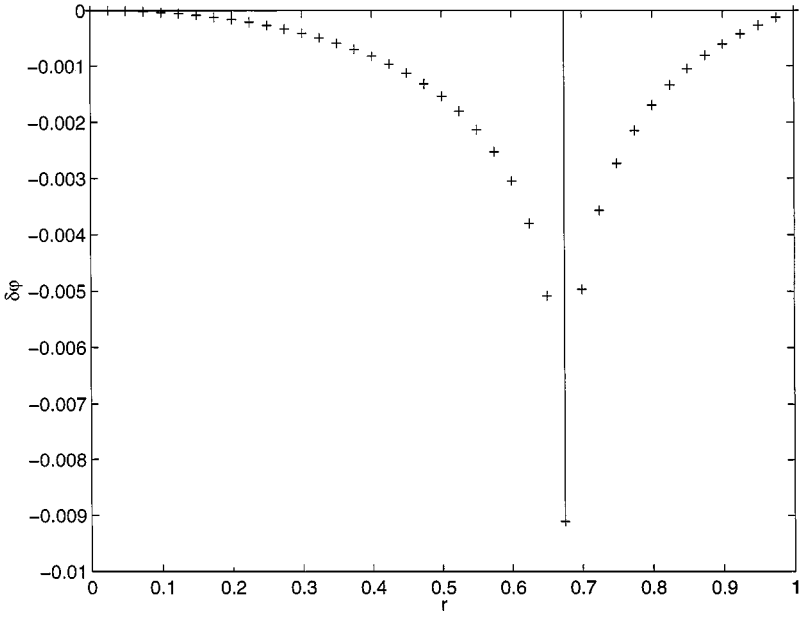

FIG. 6. Eigenfunction for $l = 2$ and $\omega = -2.61180$.

$l = 1$, 2, and 3, for values of μ in the range $0 \leq \mu \leq 1$, are shown in Fig. 7. The values for $\mu = 0$ are in agreement with Eq. (26). We observe that for both branches of the dispersion relation the frequency of the $l = 1$ mode does not vary with μ, or, in other words, the frequency depends only on the total number per unit length regardless of the profile of number density. In the low-density approximation this result has been proved for the diocotron [2]

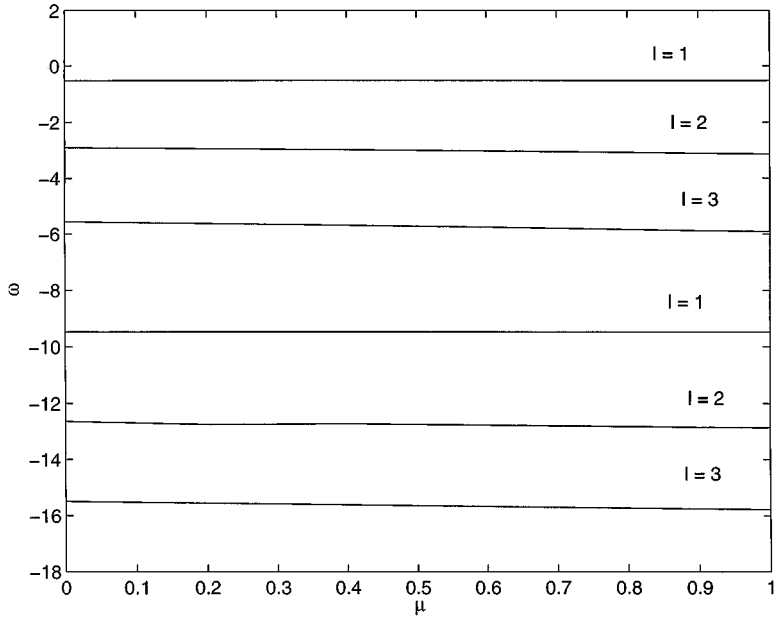

FIG. 7. Frequency of surface modes for a density profile with $M = 0.1$, $\epsilon = 1$, and $r_p = 0.5$.

as well as for the cyclotron mode [12]. The result appears to hold for a plasma of arbitrary density also. For $l = 2$ and 3 we observe an increase in the mode frequencies as μ increases, i.e., for more peaked profiles.

4.4. *Step Function Hollow Density Profile*

As a fourth test case we consider the density profile

$$n^0 = \begin{cases} 0, & 0 \le r < r_0, \\ 1, & r_0 \le r \le r_p, \\ 0, & r_p < r \le 1. \end{cases} \tag{38}$$

In the plasma region $r_0 \le r \le r_p$ the rotation frequency

$$\omega_r = \frac{-\epsilon \pm \sqrt{1 - 2M\left(1 - r_0^2/r^2\right)}}{2M}.$$

We consider $M = 0.5$, $\epsilon = 1$, $r_0 = 0.25$, and $r_p = 0.5$. The spectrum is computed for $l = 1$, $k = 0$, and 2π. These modes are found to be stable. The spectrum for $l = 2$, $k = 0$ is shown in Fig. 8. As expected the diocotron branch has an unstable mode. We also observe a complex eigenfrequency in the upper hybrid branch. The results plotted are for $N = 320$. To check whether this is a spurious unstable mode due to finite differencing we carried out calculations with $N = 40$, 80, and 160. Comparison of the imaginary part of the eigenfrequency does not show convergence to a nonzero value; rather, this part decreases

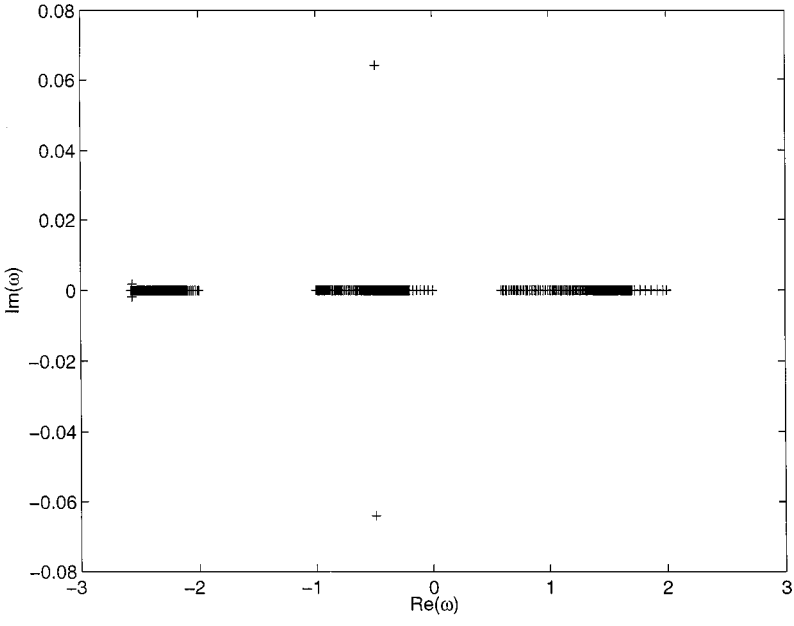

FIG. 8. The spectrum of the mode $l = 2$, $k = 0$ for a hollow density profile with $M = 0.5$, $\epsilon = 1$, $r_0 = 0.25$, and $r_p = 0.5$.

continuously with increasing N. Although we have not been able to carry out computations with sufficiently high N, where this unstable mode disappears it appears likely that this complex eigenfrequency arises due to finite differencing and does not represent an instability in the physical problem. We have also computed the spectrum for $l = 2$, $k = 2\pi$ and have observed complex eigenfrequencies which again appear to be due to finite differencing. Therefore, for a hollow density profile, for the parameters chosen in our numerical study, mode $l = 1$ is stable, mode $l = 2$, $k = 0$ has a diocotron instability, and mode $l = 2$, $k = 2\pi$ is again stable.

5. DISCUSSION

In this paper we have developed a numerical method for computing the spectrum of electrostatic modes in a cylindrical non-neutral plasma. We have used a finite difference method with a staggered grid. This allows reduction to a generalized matrix eigenvalue problem which is linear in the eigenfrequency and which can be solved using commonly available matrix eigenvalue solvers. This provides an efficient and robust method for computing the spectrum. The method has been checked using a number of test cases. Degenerate eigenvalues, sequences of eigenfrequencies, continua, and instabilities are found to be well represented by the method. The numerical code developed can be a useful tool for computing mode frequencies for cylindrical non-neutral plasmas with arbitrary number density profiles which need not satisfy the low-density approximation. The results can be useful for interpreting experimental results and for diagnostics.

The numerical code can be used to compute frequencies for cyclotron modes or for modes at the Brillouin limit where experimental observations exist [10, 33]. Earlier the observations were compared with analytical results valid for certain simple density profiles. With the code developed in this paper, mode frequencies can be computed for arbitrary profiles of the number density. Computation can be carried out for the profiles observed in the experiments.

The numerical method developed in this paper can be generalized to include more physics, e.g., plasma pressure or finite Larmor radius effects, or to multispecies ion plasmas [34]. The method can also be generalized to compute mode frequencies and instabilities in two-dimensional configurations, e.g., spheroidal or toroidal equilibria.

ACKNOWLEDGMENT

The authors thank Professor K. P. Maheshwari for his interest in the work. One of the authors (P.G.) is grateful to him for encouragement and support.

REFERENCES

1. R. H. Levy, Diocotron instability in a cylindrical geometry, *Phys. Fluids* **8**, 1288 (1965).
2. R. H. Levy, Two new results in cylindrical diocotron theory, *Phys. Fluids* **11**, 920 (1968).
3. R. J. Briggs, J. D. Daugherty, and R. H. Levy, Role of Landau damping in crossed-field electron beams and inviscid shear flow, *Phys. Fluids* **13**, 421 (1970).
4. R. C. Davidson, *An Introduction to the Physics of Nonneutral Plasmas* (Addison–Wesley, Redwood City, CA, 1990), p. 289.

5. N. R. Corngold, Linear response of the two-dimensional pure electron plasma: Quasi-modes for some model profiles, *Phys. Plasmas* **2**, 620 (1995).
6. R. L. Spencer and S. N. Rasband, Damped diocotron quasi-modes of non-neutral plasmas and inviscid fluids, *Phys. Plasmas* **4**, 53 (1997).
7. R. C. Davidson and G. M. Felice, Influence of profile shape on the diocotron instability in a non-neutral plasma column, *Phys. Plasmas* **5**, 3497 (1998).
8. P. Goswami, S. N. Bhattacharyya, A. Sen, and K. P. Maheshwari, Computation of the diocotron spectrum of a cylindrical non-neutral plasma, *Phys. Plasmas* **6**, 3442 (1999).
9. R. C. Davidson, *An Introduction to the Physics of Nonneutral Plasmas* (Addison–Wesley, Redwood City, CA, 1990), p. 240.
10. R. W. Gould and M. A. LaPointe, Cyclotron resonance in a pure electron plasma column, *Phys. Rev. Lett.* **67**, 3685 (1991); Cyclotron resonance phenomena in a pure electron plasma, *Phys. Fluids B* **4**, 2038 (1992).
11. D. L. Book, High-frequency electrostatic modes in non-neutral plasmas, *Phys. Plasmas* **2**, 1398 (1995).
12. R. W. Gould, Theory of cyclotron resonance in a cylindrical non-neutral plasma, *Phys. Plasmas* **2**, 1404 (1995).
13. D. H. E. Dubin, Theory of electrostatic fluid modes in a cold spheroidal non-neutral plasma, *Phys. Rev. Lett.* **66**, 2076 (1991).
14. J. J. Bollinger, D. J. Heinzen, F. L. Moore, W. M. Itano, D. J. Wineland, and D. H. E. Dubin, Electrostatic modes of ion-trap plasmas, *Phys. Rev. A* **48**, 525 (1993).
15. C. S. Weimer, J. J. Bollinger, F. L. Moore, and D. J. Wineland, Electrostatic modes as a diagnostic in Penning trap experiments, *Phys. Rev. A* **49**, 3842 (1994).
16. M. D. Tinkle, R. G. Greaves, C. M. Surko, R. L. Spencer, and G. W. Mason, Low-order modes as diagnostics of spheroidal non-neutral plasmas, *Phys. Rev. Lett.* **72**, 352 (1994); M. D. Tinkle, R. G. Greaves, and C. M. Surko, Low-order longitudinal modes of single-component plasmas, *Phys. Plasmas* **2**, 2880 (1995).
17. R. L. Spencer, Numerical modeling of non-neutral plasmas, in *Non-neutral Plasma Physics II* (American Institute of Physics, New York, 1995), p. 204.
18. R. L. Dewar, J. M. Greene, R. C. Grimm, and J. L. Johnson, Numerical study of the magnetohydrodynamic spectra in tokamaks using Galerkin's method, *J. Comput. Phys.* **18**, 132 (1975).
19. K. Appert, D. Berger, R. Gruber, and J. Rappaz, A new finite element approach to the normal mode analysis in magnetohydrodynamics. *J. Comput. Phys.* **18**, 284 (1975).
20. R. Gruber, Finite hybrid elements to compute the ideal magnetohydrodynamic spectrum of an axisymmetric plasma, *J. Comput. Phys.* **26**, 379 (1978).
21. R. C. Grimm, J. M. Greene, and J. L. Johnson, Computation of the magnetohydrodynamic spectrum in axisymmetric toroidal confinement systems, *Meth. Comput. Phys.* **16**, 253 (1976).
22. R. Gruber, F. Troyon, D. Berger, L. C. Bernard, S. Rousset, R. Schreiber, W. Kerner, W. Schneider, and K. V. Roberts, ERATO stability code, *Comput. Phys. Commun.* **21**, 323 (1981).
23. R. C. Grimm, R. L. Dewar, J. Manickam, S. C. Jardin, A. H. Glasser, and M. S. Chance, Resistive instabilities in tokamak geometry, in *Plasma Physics Contr. Nucl. Fusion Research 1982* (IAEA, Vienna, 1983), Vol. III, p. 35.
24. W. Kerner, Large-scale complex eigenvalue problems, *J. Comput. Phys.* **85**, 1 (1989).
25. R. C. Davidson, *An Introduction to the Physics of Nonneutral Plasmas* (Addison–Wesley, Redwood City, CA, 1990), p. 22.
26. R. C. Davidson, *An Introduction to the Physics of Nonneutral Plasmas* (Addison–Wesley, Redwood City, CA, 1990), p. 226.
27. R. C. Davidson, *An Introduction to the Physics of Nonneutral Plasmas* (Addison–Wesley, Redwood City, CA, 1990), p. 240.
28. R. C. Davidson, *An Introduction to the Physics of Nonneutral Plasmas* (Addison–Wesley, Redwood City, CA, 1990), p. 248.
29. S. N. Bhattacharyya and A. Bhattacharjee, Continuous spectrum of a non-neutral plasma column, *Phys. Plasmas* **4**, 895 (1997).

30. R. C. Davidson, *An Introduction to the Physics of Nonneutral Plasmas* (Addison–Wesley, Redwood City, CA, 1990), p. 257.
31. F. Wysocki and R. C. Grimm, A new method for computing normal modes in axisymmetric toroidal geometry using a scalar form of ideal MHD, *J. Comput. Phys.* **66**, 255 (1986).
32. K. Appert, D. Berger, R. Gruber, F. Troyon, and J. Rappaz, Studium der eigenschwingungen eines zylindrischen plasmas mit der methode der finiten elemente, *ZAMP* **25**, 229 (1974).
33. R. G. Greaves, M. D. Tinkle, and C. M. Surko, Modes of a pure ion plasma at the Brillouin limit, *Phys. Rev. Lett.* **74**, 90 (1995); M. D. Tinkle, R. G. Greaves, and C. M. Surko, Modes of spheroidal ion plasmas at the Brillouin limit, *Phys. Plasmas* **3**, 749 (1996).
34. E. Sarid, F. Anderegg, and C. F. Driscoll, Cyclotron resonance phenomena in a nonneutral multispecies ion plasma, *Phys. Plasmas* **2**, 2895 (1995).